A Tensor Framework for Alzheimer's Disease early Detection and Functional Connectivity Analysis in Resting State fMRI

Ali Noroozi, Mansoor rezghi[1,]

Department of Computer Science, Tarbiat Modares University, Tehran-Iran

Abstract

Recently machine learning methods had gain lots of publicity among researchers in order to analyze the brain images such as Resting-State Functional Magnetic Resonance Imaging(rs-fMRI) to obtain a better understanding of the brain and its related disease such as Alzheimers disease. Finding the common patterns caused by a brain disorder through analyzing the functional connectivity(FC) network along with discriminating brain diseases from normal controls have traditionally been two main goals in studying rs-fMRI data. The majority of techniques for finding an FC, calculate the FC matrix for each subject and then use simple techniques in order to combine them to obtain general functional connectivity. Also, the states of the art classification techniques for finding subjects with brain disorders, also rely on calculating an FC for each subject, vectorize them and then feed them to the classifier. Considering these problems and based on multidimensional nature data, we have come up with a novel tensor framework in which the FC calculation for each class is done without the need to construct the FC for each sample, also this framework allows us to reduce the dimensionality, and create a novel discriminant function that avoids vectorization in any step and uses the test data in the training process without forcing any prior knowledge about its label to the classifier Extensive experiments using the ADNI dataset demonstrate that our proposed framework effectively boosts the fMRI classification performance and reveals novel connectivity patterns in Alzheimer's disease at its early stages.

Email address: Rezghi@modares.ac.ir (Mansoor rezghi)

Keywords: Tensor Decomposition, fMRI, Functional Connectivity

1. Introduction

Alzheimers disease (AD) is a progressive neurodegenerative disorder with a long pre-morbid asymptomatic period which affects millions of elderly individuals worldwide[1]. It is predicted that the number of affected people will double in the next 20 years, and 1 in 85 people will be affected by 2050 [2]. The predominant clinical symptoms of AD include a decline in some important brain cognitive and intellectual abilities, such as memory, thinking, and reasoning. Precise diagnosis of AD, especially at its early warning stage: early Mild Cognitive Impairment (eMCI), enables treatments to delay or even avoid such disorders [3].

In recent years, brain imaging techniques like Positron Emission Tomography (PET)[4], Electroencephalography (EEG)[5] and functional Magnetic Resonance Imaging (fMRI)[6] have been used in the analysis of AD. Due to the high spatial resolution and relatively lower costs, fMRI is vastly used among researchers in order to monitor brain activities especially in AD and all its stages in which detecting abnormalities within small brain regions is essential [7]. An fMRI sample is naturally a 4D tensor consisting of 3D voxels moving in time, and each voxel contains an intensity value that is proportional to the strength of the Blood Oxygenation Level Dependent(BOLD) signal, which is a measure of the changes in blood flow, to estimate the activity of different brain regions[8]. Resting-state fMRI(rs-fMRI) is an fMRI technique in which the patient is asked to rest during the whole scan, focuses on the low-frequency ($< 0.1Hz$) oscillations of BOLD signal, which presents the underlying neuronal activation patterns of brain regions. rs-fMRI is usually used in order to analyze brain diseases like AD or Autism[9, 10].

Since each fMRI volume consist of hundreds of thousands of voxels which are often highly correlated with the surrounding voxels in the brain volume, parcellation of the brain for further analysis has moved toward the use of anatomical atlases. These atlases are strictly defined using anatomical features of the brain, like locations of common gyri and do not rely on any functional information. To generate data using an Atlas-based approach, the BOLD signal from all voxels is averaged within each brain region called Region of Interest(ROI)[11]. By putting together the average time-series for all the ROIs, the ith volume would become $X_i \in \mathbb{R}^{T\times R}, i = \{1, 2, \cdots, S\}$

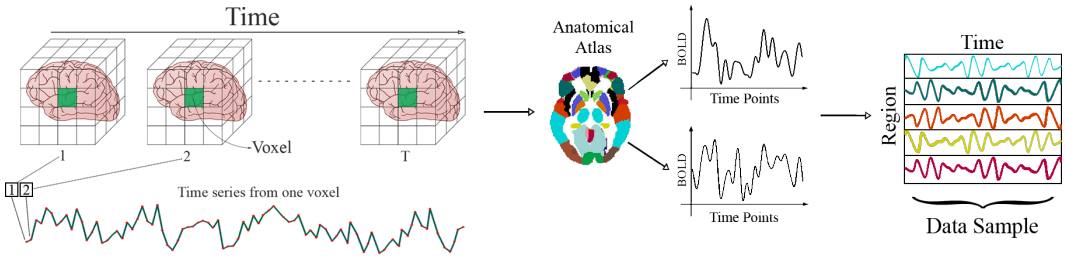

Figure 1: The process of extracting ROI time-series from the original 4D volume.

in which R, T and S are the number of ROIs, time points and samples respectively. The process of obtaining such a matrix is shown in Figure 1.

There are two major studies associated with rs-fMRI data: finding common brain disorders caused by diseases like Alzheimer's, Autism, schizophrenia and etc. and more recently detecting patients with brain disorders using classification techniques [12, 13]. Due to the high dimensionality of data and the nature of diseases like eMCI which does not show any reliable clinical symptoms, researchers moved towards advanced machine learning techniques in order to achieve more reliable analysis [14].

A powerful tool that is commonly used in order to achieve aforementioned goals is Functional Connectivity(FC) network. FC is a $region \times region$ matrix $\bar{X}$ in which $\bar{x}_{ij}$ represents the functional connectivity between the ith and jth ROI. Functional connectivity is an observable phenomenon quantifiable with measures of statistical dependencies, such as correlations, coherence, or transfer entropy [15]. Recent studies have shown that some brain disorders like AD could alter the way that some brain regions interact with each other. For example, compared with the healthy, AD patients have been found decreased functional connectivity between the hippocampus and other brain regions, and MCI patients have been observed increased functional connectivity between the frontal lobe and other brain regions[7]. So, Finding an FC that highlights the patterns caused by a disease, i.e. a **General** functional connectivity, has been a common goal in the rs-fMRI study for a long time. Several approaches exist to find common patterns among different brain scans. Data-driven methods such as PCA have been proposed for this task [16]. But ultimately most of them rely on calculating a network for each volume which may overlook the role of noises or outliers within the data[17, 18].

In recent years FCs are also used as features in classification. So, instead

of using X_i as the i^{th} sample, corresponding FC i.e. $\bar{X}_i$ is used as a feature. Although FCs show promising results, they bring their own challenges. The computational cost of FC is usually high and also its quality massively affects the performance of the learning process. Also, Since the conventional classifiers like **S**upport **V**ector **M**achine(SVM) and or k-NN works on data in vector format, these matrix features should be vectorized in order be fed to these classifiers. This vectorization leads to high-dimensional vectors which produce poor performance due to the phenomena known as the Curse of Dimensionality. Alongside the curse of dimensionality, vectorization also destroys potential information that is embedded in the structure of data. This problem has been studied especially in image data in which vectorization destroys the spatial relations within an image[19].

In this paper, based on high order tensor decomposition, we have created a framework in which the aforementioned goals i.e. finding a general FC and detecting a disorder via classification could be achieved via a single **H**igh **O**rder **S**ingular **V**alue **D**ecomposition (HOSVD) of each class. Here based on latent variables obtained by HOSVD a general representative pattern of FC for eMCI and Normal controls are obtained. The majority of connectivity patterns detected by this method have been observed and studied in several separated types of research which shows the reliability and power of the proposed method. Along with these connections, we have also detected novel connectivities especially regarding the Cerebellum which is usually discarded in the analysis of AD. The proposed classifier also outperforms state of the art eMCI classification methods.

Viewing each class as a tensor allows us to work with *time* and *region* features separately but simultaneously. This multilinear view ables us to design a proper dimension reduction relative to the nature of each feature along with a discriminant function based on linear regression on latent space of samples that uses the test data to enhance the quality of the training set without forcing any a prior knowledge to the classifier, a task which is not possible through well known classifiers like SVM, logistic regression or k-NN. It is also notable that the proposed discriminant function directly works with the X_is as features. Having the FC calculation step omitted in classification not only heavily affects the computational performance of the method, but it also saves us from the troubles of FCs which will be discussed in the next section.

To verify our approach, we conduct an extensive experimental study on

rs-fMRI data from the benchmark dataset ADNI [1]. As will be seen, the results demonstrate the effectiveness and advantages of our method. Specifically, the proposed framework, not only grants us superior classification accuracy to that from other methods, but it is also much faster and more stable against different data selection schemes. We have also confirmed our achieved general FC matrix using empirical data on the eMCI and Normal functional connectivity patterns.

2. eMCI classification and FC construction techniques

As it was mentioned before, obtaining and classifying FC matrices have become the dominant approach towards eMCI analysis. Variety of methods such as Pairwise Pearsons correlation coefficient [20, 21], sparse representation [20, 22, 23] and **S**parse **I**nverse **C**ovariance **E**stimation (SICE)[24] exists to obtain an FC. While the first two are easy to understand and can capture pairwise functional relationship based on a pair of ROIs, the latter can account for more complex interactions among multiple ROIs, but the estimation of partial correlation involves an inversion of a covariance matrix, which may be ill-posed due to the singularity of the covariance matrix. These methods result in vastly different networks[12]. On the other hand, computing the correlations, based on the entire time series of fMRI data simply measures the FC between ROIs with a scalar value, which is fixed across time. This actually implicitly hypothesizes the **Stationary** interaction patterns among ROIs which will result in a *static functional connectivity* (sFC). As a result, this method may overlook the complex and dynamic interaction patterns among ROIs, which are essentially time-varying. In order to overcome this issue, **Non-stationary** methods have been proposed which results in more complex networks also known as dynamic functional connectivity (dFC)[25, 26, 27]. The most common and straightforward way to investigate dFC is using windowed FC, which consists of calculating a given FC measure, for example, the Pearson correlation coefficient, over consecutive windowed segments of the data[28, 29]. Although such an analysis seems straightforward, there are also pitfalls associated with it which may cause in a non-accurate FC[30].

In the following, we briefly discuss two states of the art eMCI classification techniques belonging to these two paradigms:

[1] http://adni.loni.usc.edu/

Kernel Compact SICE($\mathbf{K-SIEC}$) : SICE matrix have proven itself to be one of the best static functional connectivity models [24, 19, 31, 32, 33], which is extracted via the following optimization:

$$S^* = \arg\max_{S \succ 0} \quad \log\left(\det(S)\right) - \mathrm{tr}(CS) - \lambda \left\|S\right\|_1 \tag{1}$$

where C is the sample-based covariance matrix; det(), tr(), and $\|.\|_1$ denote the determinant, trace, and the sum of the absolute values of the entries of a matrix respectively. In classification with FC features, the vectorized SICE of each sample is used [26]. The occurrence of the curse of dimensionality and losing useful information contained in the SICE matrices(like SPD property) are two main drawbacks of this vectorization approach. To overcome these drawbacks, since each SICE matrix belongs to symmetric semidefinite positive definite (SPD) matrices Riemannian manifold, in the proposed method in [34], some SPD manifold-based distances like Log-Euclidean distance[35] and Root Stein divergence[36] are employed in kernel-based PCA to extract a compact representation of brain network. The power of this method resides in a massive dimension reduction of SICE, using its SPD property. The performance of this method heavily relies on the choice of sparsity parameter λ for SICE calculations and the number of top eigenvectors m.

High Order Networks(**HON**) : This method which is proposed in [37], belongs to non-stationary paradigm and uses the so called High Order Networks as features for classification purposes. It uses the sliding window technique in order to split the time-series into smaller pieces and then find the relation between them[38, 39, 40]. Let $x_i^{(l)}(k) \in \mathbb{R}^N$ denotes the k-th segment of the i-th region in the l-th sample. For each sample a network with nodes $x_i^{(l)}(k)$ could be constructed which its edge weights are obtained as

$$C_{ij}^{(l)}(k) = \mathrm{corr}\left(x_i^{(l)}(k), x_j^{(l)}(k).\right)$$

Here the weight $C_{ij}^{(l)}(k)$ represents the pairwise Pearsons correlation coefficients between the i-th and the j-th ROIs of the l-th subject using the k-th segment of subseries. Now

$$y_{ij}^{(l)} = \left[C_{ij}^{(l)}(1), C_{ij}^{(l)}(2), \cdots, C_{ij}^{(K)}(1)\right] \in \mathbb{R}^K$$

represents the similarity of the ith and j-th, regions of the l-th sample in all segments. for each l by considering $y_{ij}^{(l)}$ as nodes of a networks with weights

$$H_{ij,pq}^{(l)} = \mathrm{corr}\left(y_{ij}^{(l)}, y_{pq}^{(l)}\right)$$

an higher-order network is obtained for each sample. Here for each pair of correlation time series y_{ij} and y_{pq}, $H^{(l)}_{ij,pq}$ indicates how the correlation between the i-th and the j-th ROIs influence the correlation between the p-th and the q-th ROIs. So for each sample its higher-order networks $\{H^{(l)}_{ij,pq}\}$ will be a matrix with size $R^4 \times R^4$(R is the number of regions) which will lead to a large-scale high-order FC network, containing at least thousands of vertices and millions of edges. In order to overcome this issue, the correlation time series within each subject are grouped into different clusters. Then, the correlation computations are carried out between the means of clusters. After reducing the network size, the weighted-graph local clustering coefficients was used to select the key features for each network and then an SVM classifier is trained in order to classify the obtained features. As a result of constructing a high-order network, the notion of a physical ROI become vague and thus such networks are not preferable choices in order to analyze functional connectivities.

It is noteworthy that none of these techniques consider the multi-linearity nature of the data, and since both methods use traditional classifiers like SVM or KNN, they follow a rather complex path to find vector features as the representative of each FC matrix.

3. Proposed fMRI analysis Framework Based On HOSVD

(

4. EXPERIMENTAL STUDY

4.1. Data Preprocessing and Experimental Settings

Rs-fMRI data of 196 subjects were downloaded from the ADNI website[2]. Nine subjects were discarded due to the corruption of data, and the remaining 187 subjects were preprocessed for analysis. After removing subjects that had problems in the preprocessing steps, such as large head motion, 156 subjects were kept, including 26 AD, 44 early MCI, 38 late MCI, 38 NC, and ten significant memory concern labeled by ADNI. We used the 38 NC and the 44 early MCI because our focus in this paper is to identify MCI at a very early stage, which is the most challenging and significant task in AD prediction.

[2]http://adni.loni.usc.edu

The IDs of the 82 (38 NC and 44 early MCI) subjects are provided in the supplementary material.

The data are acquired on a 3-T (Philips) scanner with TR/TE set as 3000/30 ms and flip angle of 80. Each series has 140 volumes, and each volume consists of 48 slices of image matrices with dimensions 64×64 with voxel size of $3.31 \times 3.31 \times 3.31\ mm^3$. The preprocessing is carried out using SPM12 and DPARSFA [43]. The first ten volumes of each series are discarded for signal equilibrium. Slice timing, head motion correction, and MNI space normalization are performed. Participants with too much head motion are excluded. The normalized brain images are warped into automatic anatomical labeling (AAL) [44] atlas to obtain 116 ROIs as nodes. By following common practice [45, 46, 47], the ROI mean time series are extracted by averaging the time series from all voxels within each ROI and then bandpass filtered to obtain multiple sub-bands as in [47].

4.2. Classification

Almost every subject in ADNI dataset has several scans. Usually, random scan data is selected and enters the processing step[34]. This random selection may cause several problems. Since the number of train data is very low, a small alteration in the samples could drastically change the set of input parameters in order to achieve the highest prediction accuracy and other classification evaluation methods. Also achieving high-quality results with a classifier does not guarantee its effectiveness on other datasets even with fine-tuning the parameters since the training set may contain outliers and unidentified corrupted data.

In order to show that the proposed framework is less sensitive against the choice of different permutations of data (i.e. Same patient with the different scan) is less vulnerable towards the aforementioned issues, we have selected 18 different permutations of data and test two state of the art classification methods on them: **HON** and **k-SICE**. To make full use of the limited subjects, a leave-one-out procedure is used for training and test. That is, each sample is reserved for the test in turn, while the remaining samples are used for training. We have use five evaluation measures: accuracy (ACC), sensitivity (SEN), Youdens index(YI), F-score, and balanced accuracy (BAC)[48].

In this article, we treat the eMCI samples as positive class and the NC samples as negative class.

Table 1: The Average of Different Classification Measurements in all dataset permutations in %

Method	ACC	F-Score	SEN	SPE	YI	BAC
k-SICE	75.57	77.36	78.50	72.19	50.69	75.34
FON	75.66	77.44	78.40	72.48	50.89	75.44
Proposed	**80.43**	**82.20**	**84.60**	**75.59**	**60.20**	**80.09**

4.2.1. Classification performance

The classification accuracy measure(ACC), After fine-tuning the input parameter set for each method, shows that for 16 out of 18 different random selected datasets, our approach performs better than k-SICE, the same also holds for 15 datasets comparing to HON. i.e. in 88.8% of datasets, proposed method works better than k-SICE and in 83.3% of datasets, it works better than FON. The highest classification accuracy(86.59%) is achieved with the proposed method in the 15th sample data. The highest accuracy for the HON (84.15%) is achieved in the 14th, and the highest accuracy for the SICE method (85.37%) is achieved in the 6th sample data. As it was mentioned before, being stable when the input dataset changes is a very important aspect for a classifier, in order to measure the stability, the standard deviation of accuracy along with other measures are calculated. The std. of accuracy for the proposed method is 0.64 times less than HON and 1.73 times less than k-SICE method. Similar results also hold for other classification measures.

Figure (2) shows the performance of these three methods in all five measurements. Some statistical information about these plots is also included in the embedded table. As it can bee seen in this figure, similar to the accuracy, the proposed method in overall works much better than FON and k-SICE. For a better Demonstration, table (1) provides the average of several classification measurements scores for all dataset permutations. As it can be seen in this table, the average accuracy of Proposed method which is 80.43% is 4.77% higher than the next method HON, and 4.86% better than k-SICE. It is noteworthy that The other two methods i.e HON and SICE shows similar results in average.

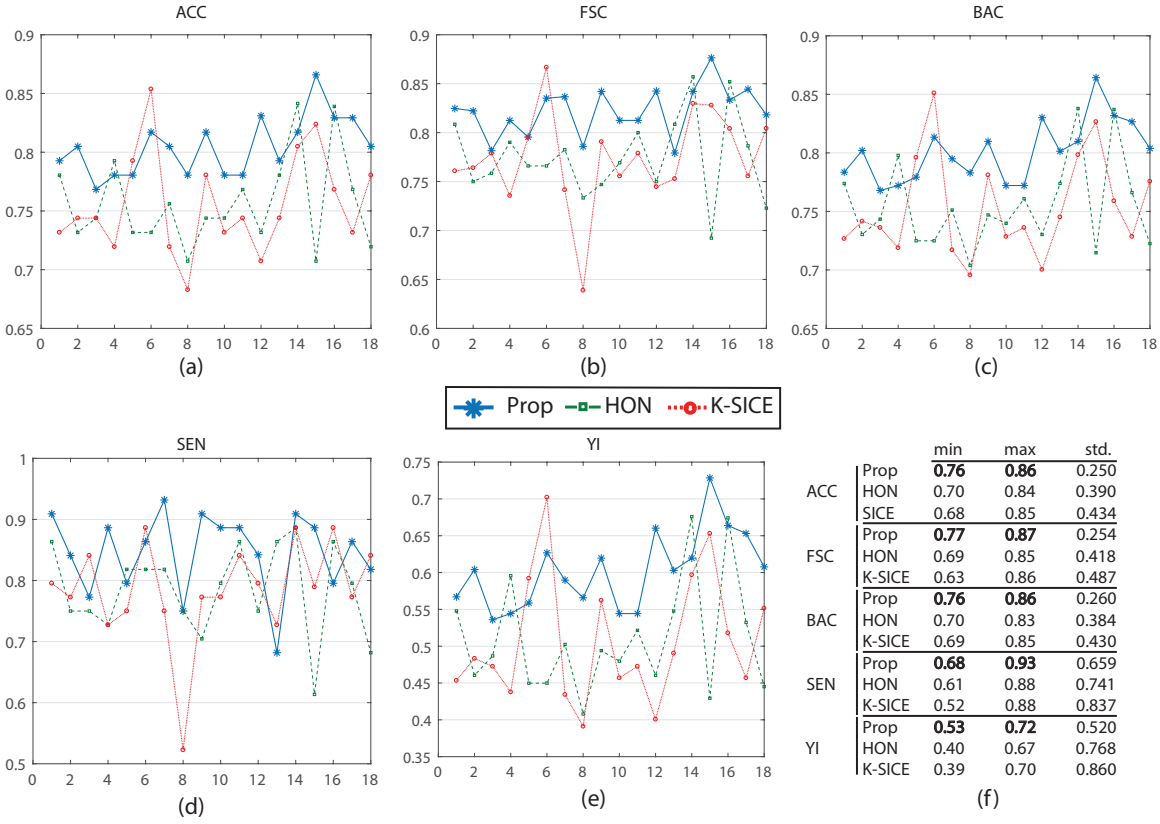

		min	max	std.
ACC	Prop	**0.76**	**0.86**	0.250
	HON	0.70	0.84	0.390
	SICE	0.68	0.85	0.434
FSC	Prop	**0.77**	**0.87**	0.254
	HON	0.69	0.85	0.418
	K-SICE	0.63	0.86	0.487
BAC	Prop	**0.76**	**0.86**	0.260
	HON	0.70	0.83	0.384
	K-SICE	0.69	0.85	0.430
SEN	Prop	**0.68**	**0.93**	0.659
	HON	0.61	0.88	0.741
	K-SICE	0.52	0.88	0.837
YI	Prop	**0.53**	**0.72**	0.520
	HON	0.40	0.67	0.768
	K-SICE	0.39	0.70	0.860

(f)

Figure 2: Comparison of proposed method(Prop) with K-SICE and HON applied on 18 different dataset permutations in five different classification evaluation measures. Figures *a* through *e* shows *accuracy*, *F-Score*, *balanced accuracy*, *sensitivity* and *Youden Index* respectively along with the max, min and standard deviation of each one presented at the embedded table (f).

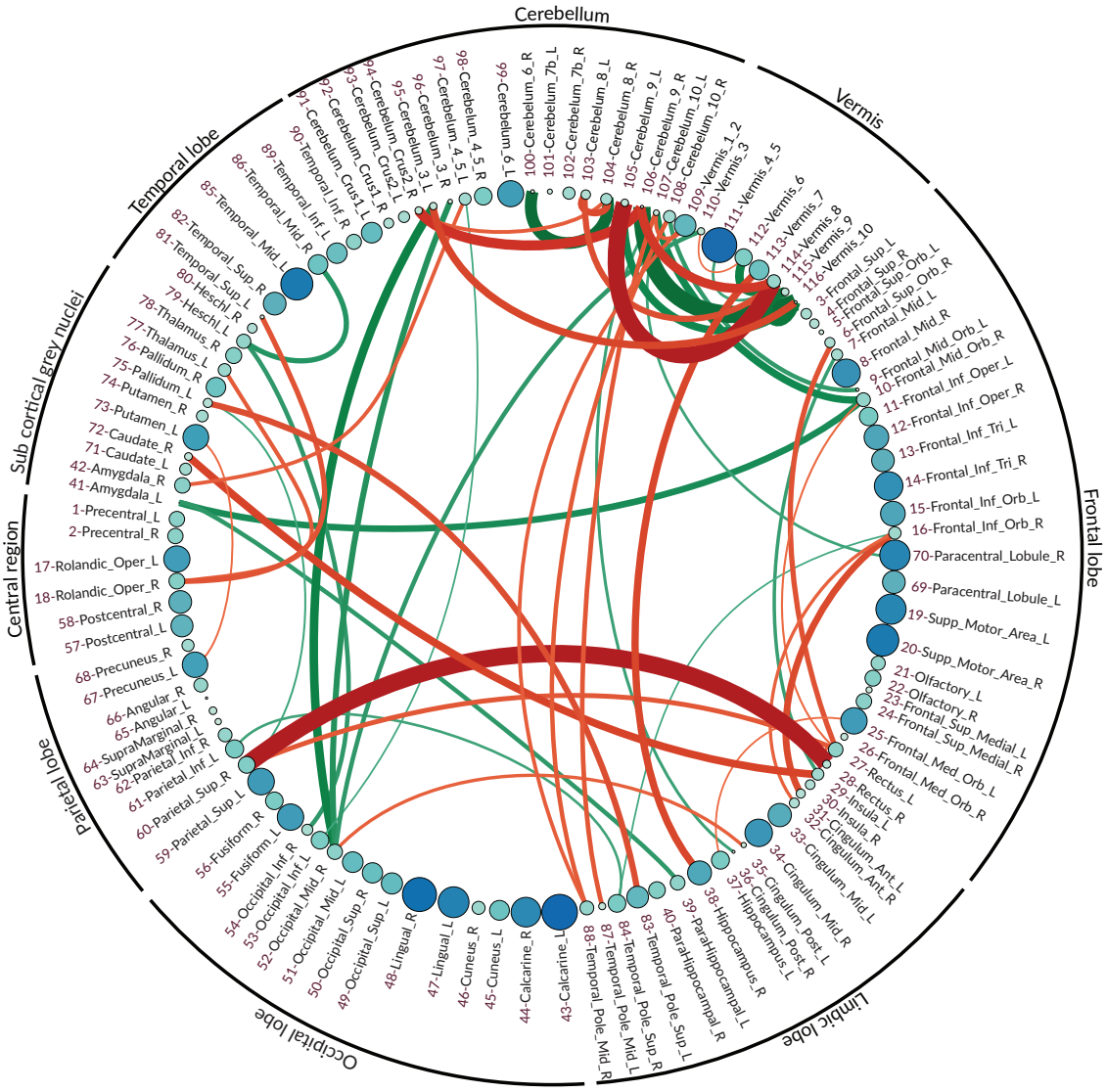

Figure 3: The difference graph. This graph is obtained via subtracting the functional connectivity of eMCI subjects from normal subjects. Each circle represents a ROI in AAL atlas and the color and size of each circle is proportional to the graph clustering coefficient of the difference graph. red = more activity in EMCI, green: less.

Table 2: Elapsed time of the test and train phase in seconds

Method	HON	k-SICE	proposed method
Elapsed Time	6950	230	11

4.2.2. Runtime Comparison

One other key features of the proposed method is that it works significantly faster than the other two methods. Table (2) shows the average elapsed time (Training plus Testing) of each method for all data permutations. These methods were executed in Matlab R2017b and carried with an Intel Core-i7 processor and 16GB of RAM. As it can be seen in this table, the proposed method is more than 600 times faster than HON and 20 times faster that SICE. Having a huge execution time especially affects the parameter selection for HON, since it uses cross-validation procedure in order to find the optimal parameters which itself require several runs of the algorithm.

4.3. Functional connectivity Network

The vector features for both Normal and eMCI classes was obtained via the proposed method as it is described in (3.2). Due to the aforementioned qualities of partial correlation, SICE is deployed in order to obtain the final FC. In order to better highlight the differences between Normal and eMCI subjects, a difference graph D is constructed by subtracting the Normal FC from the eMCI FC. This graph could be seen in Figure(3). The nodes of D shows the ROIs according to the AAL atlas. The size of each node is proportional to its graph clustering coefficient, i.e. the bigger node demonstrates higher activity in eMCI subjects in the corresponding ROI. Similar to nodes, the size of each edge is also proportional to the correlation between two ROI's. In addition, the edges are also color-coded in a way that the green edges show the positive edges in D and the orange edges shows the negative edges in D. In this manner, the green edges demonstrate decreasing in activity between the corresponding nodes in eMCI subjects and vice versa, the orange edges shows increasing activity between corresponding ROIs in the eMCI subjects.

As it can be seen in the difference graph, the big nodes i.e. ROIs with higher activities does not necessarily establish strong connections with the other nodes. As an obvious example, higher activities in Lingual gyrus(ROI

index: 47,48)[49], Calcarine sulcus(ROI index: 43, 44)[50, 51], Supplementary motor area(ROI index: 19,20)[51, 52] and Temporal_mid_L(ROI index: 85)[53] are easily detectable. The majority of ROIs located in frontal lobe also shows rather high activities comparing to normal subjects[54, 7].

Similar to the nodes, the strong edge between two ROIs does not necessarily require the nodes to be highly active in eMCI. Although a strong edge does indicate high activities and functional connectivity between the two corresponding ROIs. The difference Graph shows a significant increase in connectivity between Rectus(ROI index: 28, 27 in Frontal lobe) and Parietal_Sup_R(ROI index: 60 in Parietal lobe) [55, 56], Frontal_Inf_Orb_R(ROI index: 16 in Frontal lobe) and Cingulum_Ant(ROI index: 31,32 in Limbic lobe)[57], Insula_L, Temporal_Pole_Sup_L(ROI index: 29,83 in Limbic lobe) and Pallidum_R, Caudate_R(ROI index: 29,83 in Sub Cortical Grey Nuclei)[58]. It can also be seen that within activities in frontal lobe also increased in patients with eMCI[59]. There is a decrease in connectivity between Amygdala_L(ROI index: 41 in Sub Cortical Grey Nuclei) with Frontal_Mid_Orb_R(ROI index: 10 in Sub Frontal lobe) and ParaHippocampal_L(ROI index: 39 in Sub Limbic lobe)[60]. The connectivity between Heschl_L(ROI index: 79 in Temporal lobe) and two ROIs Temporal_Mid_R(ROI index: 86 also in Temporal lobe) and Occipital_Inf_R(ROI index: 54 in Occipital lobe) also decreased in eMCI[61].

Regarding the Cerebellum and Vermis

In fMRI data analysis and especially in Alzheimer's disease studies, ROIs within the Cerebellum and Vermis are usually excluded since their role was regarded as insignificant[62, 63]. Recent studies have shown that the traditional assumption that Cerebral area is essential only for the coordination of voluntary motor activity and motor learning is not valid and indicates the significant role of the cerebellum in nervous system function, cognition, and emotion[64].

As it can be seen in the difference graph that we obtained, ROIs within Cerebellum and Vermis are highly active and both their Intra and interconnections are noticeable. There is increased functional connectivity between the Limbic lobe especially Hippocampus_R, Temporal_Pole_Mid(ROI index: 38,87,88) and Cerebral areas in eMCI patients. Also, the connectivity between Occipital lobe, especially Occipital_mid_R(ROI index: 52), the Frontal lobe, especially in Frontal_mid_orb(ROI index: 9,10) and Cerebral areas seems to decrease in patients with eMCI.

5. Conclusion

The majority of functional connectivity analysis methods rely on calculating the FC matrix for each individual, then using simple methods to combine them in order to obtain a general FC network for a class. Also, the state of the art classification techniques use FC as the representative for each sample. In this paper, based on multilinear nature of data, we have proposed a novel framework in which the general FC is extracted directly from the Time-Region features and does not rely on individual FC calculations. Also the obtained FC by the proposed method contains some relations that recently approved experimentally. This framework also ables us to design a discriminant function that works directly with $Time \times Region$ samples rather that their FC. The new discriminant function also uses the test data in order to enhance the training set. The benefits of the proposed method could be summarize as follow: Extensive studies on the rs-fMRI provided by ADNI shows the superiority of the proposed framework in both classification and functional connectivity. The obtained FC network not only acknowledge the previous discovered connections but also reveals new connectivity patterns previously unknown. The framework proposed in this paper can be easily extended to other studies involved with high order data.

References

[1] Caselli, Richard J., et al. "Longitudinal changes in cognition and behavior in asymptomatic carriers of the APOE e4 allele." Neurology 62.11 (2004): 1990-1995.

[2] Brookmeyer, Ron, et al. "Forecasting the global burden of Alzheimers disease." Alzheimer's & dementia: the journal of the Alzheimer's Association 3.3 (2007): 186-191.

[3] Musha, Toshimitsu, et al. "EEG markers for characterizing anomalous activities of cerebral neurons in NAT (neuronal activity topography) method." IEEE Transactions on Biomedical Engineering 60.8 (2013): 2332-2338.

[4] Nordberg, Agneta. "PET imaging of amyloid in Alzheimer's disease." The lancet neurology 3.9 (2004): 519-527.

[5] Jeong, Jaeseung. "EEG dynamics in patients with Alzheimer's disease." Clinical neurophysiology 115.7 (2004): 1490-1505.

[6] Golby, Alexandra, et al. "Memory encoding in Alzheimer's disease: an fMRI study of explicit and implicit memory." Brain 128.4 (2005): 773-787.

[7] Dennis, Emily L., and Paul M. Thompson. "Functional brain connectivity using fMRI in aging and Alzheimers disease." Neuropsychology review 24.1 (2014): 49-62.

[8] R. Graaf and K. Kevin. Methods and apparatus for compensating eld inhomogeneities in magnetic resonance studies. US Patent No. 8035387, 2011.

[9] N. Leonardi et al., Principal components of functional connectivity: A new approach to study dynamic brain connectivity during rest, NeuroImage, vol. 83, pp. 937950, 2013.

[10] Cherkassky, Vladimir L., et al. "Functional connectivity in a baseline resting-state network in autism." Neuroreport 17.16 (2006): 1687-1690.

[11] Stanley, Matthew Lawrence, et al. "Defining nodes in complex brain networks." Frontiers in computational neuroscience 7 (2013): 169.

[12] Du, Yuhui, Zening Fu, and Vince D. Calhoun. "Classification and prediction of brain disorders using functional connectivity: promising but challenging." Frontiers in neuroscience 12 (2018).

[13] de Vos, Frank, et al. "A comprehensive analysis of resting state fMRI measures to classify individual patients with Alzheimer's disease." Neuroimage 167 (2018): 62-72.

[14] Cuingnet, Rmi, et al. "Automatic classification of patients with Alzheimer's disease from structural MRI: a comparison of ten methods using the ADNI database." neuroimage 56.2 (2011): 766-781.

[15] Friston, Karl J. "Functional and effective connectivity: a review." Brain connectivity 1.1 (2011): 13-36.

[16] Leonardi, Nora, et al. "Principal components of functional connectivity: a new approach to study dynamic brain connectivity during rest." NeuroImage 83 (2013): 937-950.

[17] Supekar, Kaustubh, et al. "Network analysis of intrinsic functional brain connectivity in Alzheimer's disease." PLoS computational biology 4.6 (2008): e1000100.

[18] Contreras, Joey A., et al. "Resting state network modularity along the prodromal late onset Alzheimer's disease continuum." NeuroImage: Clinical 22 (2019): 101687.

[19] Ahmadi, Soheil, and Mansoor Rezghi. "A novel extension of Generalized Low-Rank Approximation of Matrices based on multiple-pairs of transformations." CoRR (2018).

[20] Jie, Biao, et al. "Integration of network topological and connectivity properties for neuroimaging classification." IEEE transactions on biomedical engineering 61.2 (2014): 576-589.

[21] Wee, Chong-Yaw, et al. "Resting-state multi-spectrum functional connectivity networks for identification of MCI patients." PloS one 7.5 (2012): e37828.

[22] Tibshirani, Robert, et al. "Sparsity and smoothness via the fused lasso." Journal of the Royal Statistical Society: Series B (Statistical Methodology) 67.1 (2005): 91-108.

[23] Wright, John, et al. "Robust face recognition via sparse representation." IEEE transactions on pattern analysis and machine intelligence 31.2 (2009): 210-227.

[24] Huang, Shuai, et al. "Learning brain connectivity of Alzheimer's disease by sparse inverse covariance estimation." NeuroImage 50.3 (2010): 935-949.

[25] Allen, Elena A., et al. "Tracking whole-brain connectivity dynamics in the resting state." Cerebral cortex 24.3 (2014): 663-676.

[26] Leonardi, Nora, et al. "Principal components of functional connectivity: a new approach to study dynamic brain connectivity during rest." NeuroImage 83 (2013): 937-950.

[27] Leonardi, Nora, and Dimitri Van De Ville. "On spurious and real fluctuations of dynamic functional connectivity during rest." Neuroimage 104 (2015): 430-436.

[28] Barttfeld, Pablo, et al. "Signature of consciousness in the dynamics of resting-state brain activity." Proceedings of the National Academy of Sciences 112.3 (2015): 887-892.

[29] Zalesky, Andrew, et al. "Time-resolved resting-state brain networks." Proceedings of the National Academy of Sciences 111.28 (2014): 10341-10346.

[30] Hindriks, Rikkert, et al. "Can sliding-window correlations reveal dynamic functional connectivity in resting-state fMRI?." Neuroimage 127 (2016): 242-256.

[31] Ng, Bernard, et al. "A novel sparse group Gaussian graphical model for functional connectivity estimation." International Conference on Information Processing in Medical Imaging. Springer, Berlin, Heidelberg, 2013.

[32] Colclough, Giles L., et al. "Multi-subject hierarchical inverse covariance modelling improves estimation of functional brain networks." NeuroImage 178 (2018): 370-384.

[33] Foti, Nicholas J., and Emily B. Fox. "Statistical model-based approaches for functional connectivity analysis of neuroimaging data." Current opinion in neurobiology 55 (2019): 48-54.

[34] Zhang, Jianjia, et al. "Functional brain network classification with compact representation of SICE matrices." IEEE Transactions on Biomedical Engineering 62.6 (2015): 1623-1634.

[35] V.Arsigny et al.,. (2006). Log-euclidean metrics for fast and simple calculus on diffusion tensors. Magn. Reson. Med.. [Online]. 56(2), pp. 411421. Available: http://dx.doi.org/10.1002/mrm.20965

[36] S. Sra, A new metric on the manifold of kernel matrices with application to matrix geometric mean, in Advances in Neural Information Processing Systems 25, F. Pereira, C. J. C. Burges, L. Bottou, K. Q.Weinberger, Eds., New York, NY: Curran Associates, Inc., 2012, pp. 144152.

[37] Chen, Xiaobo, et al. "Highorder restingstate functional connectivity network for MCI classification." Human brain mapping 37.9 (2016): 3282-3296.

[38] Allen, Elena A., et al. "Tracking whole-brain connectivity dynamics in the resting state." Cerebral cortex 24.3 (2014): 663-676.

[39] Chang, Catie, and Gary H. Glover. "Timefrequency dynamics of resting-state brain connectivity measured with fMRI." Neuroimage 50.1 (2010): 81-98.

[40] Handwerker, Daniel A., et al. "Periodic changes in fMRI connectivity." Neuroimage 63.3 (2012): 1712-1719.

[41] Ye, Jieping. "Generalized low rank approximations of matrices." Machine Learning 61.1-3 (2005): 167-191.

[42] Rezghi, Mansoor. "A novel fast tensor-based preconditioner for image restoration." IEEE Transactions on Image Processing 26.9 (2017): 4499-4508.

[43] Yan, Chaogan, and Yufeng Zang. "DPARSF: a MATLAB toolbox for" pipeline" data analysis of resting-state fMRI." Frontiers in systems neuroscience 4 (2010): 13.

[44] Tzourio-Mazoyer, Nathalie, et al. "Automated anatomical labeling of activations in SPM using a macroscopic anatomical parcellation of the MNI MRI single-subject brain." Neuroimage 15.1 (2002): 273-289.

[45] S. M. Smith et al., Functional connectomics from resting-state fMRI, Trends Cognit. Sci., vol. 17, no. 12, pp. 666682, 2013.

[46] N. Leonardi et al., Principal components of functional connectivity: A new approach to study dynamic brain connectivity during rest, NeuroImage, vol. 83, pp. 937950, 2013.

[47] C.-Y. Wee et al., Constrained sparse functional connectivity networks for MCI classification, in Proc. Med. Image Comput. Comput.-Assisted Intervention Conf., 2012, pp. 212219.

[48] Tan, Pang-Ning. Introduction to data mining. Pearson Education India, 2018.

[49] He, Yong, et al. "Regional coherence changes in the early stages of Alzheimers disease: a combined structural and resting-state functional MRI study." Neuroimage 35.2 (2007): 488-500.

[50] Bakkour, Akram, et al. "The effects of aging and Alzheimer's disease on cerebral cortical anatomy: specificity and differential relationships with cognition." Neuroimage 76 (2013): 332-344.

[51] Brewer, Alyssa A., and Brian Barton. "Visual cortex in aging and Alzheimer's disease: changes in visual field maps and population receptive fields." Frontiers in psychology 5 (2014): 74.

[52] Jacobsen, Jrn-Henrik, et al. "Why musical memory can be preserved in advanced Alzheimers disease." Brain 138.8 (2015): 2438-2450.

[53] Kosicek, Marko, and Silva Hecimovic. "Phospholipids and Alzheimers disease: alterations, mechanisms and potential biomarkers." International journal of molecular sciences 14.1 (2013): 1310-1322.

[54] Salvatore, Christian, et al. "Magnetic resonance imaging biomarkers for the early diagnosis of Alzheimer's disease: a machine learning approach." Frontiers in neuroscience 9 (2015): 307.

[55] Brickman, Adam M., et al. "Reconsidering harbingers of dementia: progression of parietal lobe white matter hyperintensities predicts Alzheimer's disease incidence." Neurobiology of aging 36.1 (2015): 27-32.

[56] De Reuck, J., et al. "Topography of cortical microbleeds in Alzheimers disease with and without cerebral amyloid angiopathy: a post-mortem 7.0-tesla MRI Study." Aging and disease 6.6 (2015): 437.

[57] Perani, Daniela, et al. "The impact of bilingualism on brain reserve and metabolic connectivity in Alzheimer's dementia." Proceedings of the National Academy of Sciences 114.7 (2017): 1690-1695.

[58] Watson, Rosie, et al. "Subcortical volume changes in dementia with Lewy bodies and Alzheimer's disease. A comparison with healthy aging." International psychogeriatrics 28.4 (2016): 529-536.

[59] Cai, Suping, et al. "Changes in thalamic connectivity in the early and late stages of amnestic mild cognitive impairment: a resting-state functional magnetic resonance study from ADNI." PloS one 10.2 (2015): e0115573.

[60] Ortner, Marion, et al. "Progressively Disrupted intrinsic Functional connectivity of Basolateral amygdala in Very early alzheimers Disease." Frontiers in neurology 7 (2016): 132.

[61] Steketee, Rebecca ME, et al. "Early-stage differentiation between presenile Alzheimers disease and frontotemporal dementia using arterial spin labeling MRI." European radiology 26.1 (2016): 244-253.

[62] Sanz-Arigita, Ernesto J., et al. "Loss of small-worldnetworks in Alzheimer's disease: graph analysis of FMRI resting-state functional connectivity." PloS one 5.11 (2010): e13788.

[63] Zhang, Daoqiang, et al. "Multimodal classification of Alzheimer's disease and mild cognitive impairment." Neuroimage 55.3 (2011): 856-867.

[64] Jacobs, Heidi IL, et al. "The cerebellum in Alzheimers disease: evaluating its role in cognitive decline." Brain 141.1 (2017): 37-47.